High Resolution QWIP and T2SL IDDCAs by IRnova

W. Diel[1], M. Pozzi[1], D. Evans[1], J. Alverbro[1], S. Naureen[1], L. Höglund[1], M. Fawakhiri[1]
S. Bae[2], E. Costard[1]
[1] IRnova AB, Electrum 236, Kista, Sweden, SE-164 40
[2] i3System, Inc. 26-32 Gajeongbuk-ro, Yuseong-gu, Daejeon, Republic of Korea (305-343)

ABSTRACT

Lately IRnova's research activities have been focused on the development of its next generation Type II Superlattice (T2SL) and Quantum Well Infrared Photodetector (QWIP) based infrared focal plane arrays (FPA) and Integrated Detector Dewar Cooler Assembly (IDDCAs) with 640×512 pixels @ 15µm pixel pitch. Last year we presented the initial results obtained for both of the above mentioned technologies at FPA and single element level. In this paper we will introduce our next generation of fully functional IDDCA (@15µm pixel pitch) solutions for MWIR and LWIR detection based on T2SL and QWIP technology respectively. Novelty of these IDDCAs lies in that fact that both of these products make use of FLIR indigo's ISC0403, and similar Cooler & Dewar assemblies. Performance in terms of picture quality, operability, response uniformity, stability and NETD of these IDDCAs is evaluated using demonstrator cameras developed in-house. This QWIP based LWIR IDDCA is the smallest pixel pitch commercially available IDDCA using this technology.

Keywords: T2SL, QWIP, MWIR, LWIR, IDDCA

1. INTRODUCTION

IRnova has developed its next generation IDDCAs, keeping in mind the needs for the next generation of IR detectors like large format, uniformity, gain stability and agile pixels and to address varying customer requirements based on object to be detected under different atmospheric conditions. For the MWIR waveband we make use of the new T2SL technology and to address the LWIR waveband we make use of the QWIP technology that is proven for its robustness.

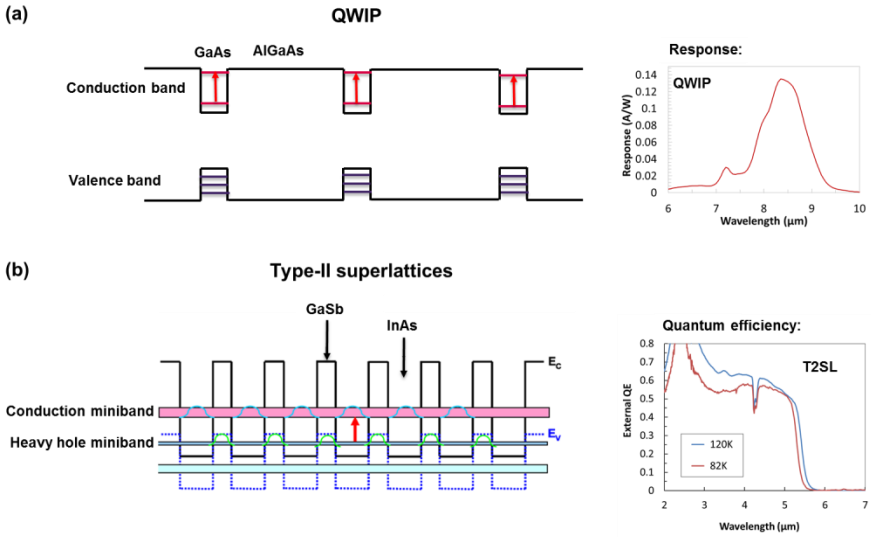

Figure 1. The two different detector technologies used at IRnova: (a) QWIP detectors which are based on intersubband transitions which generate narrow band response (b) T2SL detectors which are based on interband transitions with broadband response.

In previous publications, the performance of our LWIR [1] and MWIR [2] FPAs were demonstrated for different formats (384×288, 320×256 and 640×512). Last year, we presented our work on high resolution (640×512) QWIP photodetector with a pixel pitch of 15µm [3], which contradicted the conventional belief that the pixel pitch of an LWIR waveband QWIP is limited to ~19µm. We have successfully developed this FPA format with excellent results, and also integrated this FPA in our now commercially available IDDCA. The small pitch development was based on the initial studies done by Nedelcu et.al. [4] and their recent work [5].
This article focuses on our 640- LW IDDCA (640×512 @ 15µm pixel pitch) based on QWIP technology and we will also show the performance results from our 640- MW IDDCA based on T2SL technology. First, the experimental details are described highlighting the process used for FPA fabrication. Following this, the details of the IDDCA manufacturing process will be presented. In the results section the performances of the IRnova 640-LW IDDCA (LWIR waveband) and IRnova 640-MW IDDCA (MWIR waveband) are evaluated in terms of Noise Equivalent Temperature Difference (NETD), Modulation Transfer Function (MTF) measured using slanted edge method and Fixed Pattern Noise (FPN) measured using the two-point non-uniformity correction from one thermal cycle to another and stability over time.

2. EXPERIMENTAL DETAILS

2.1. Fabrication

Complete FPA production for both QWIPs and T2SLs is divided into four phases, Material validation, Wafer process, Hybridization (flip-chip bonding of detector arrays with the ROICs), FPA characterization in test Dewar.

GaAs/AlGaAs based QWIP wafers used for LWIR detectors were grown using metal-organic vapour phase epitaxy (MOVPE) reactor on 100 mm GaAs wafer. Details of the growth parameters can be found in [1]. Whereas InAs/GaSb based T2SL wafers for MWIR detectors were grown using molecular beam epitaxy (MBE), details of the material design and device results can be found in [6].

For wafer processing, QWIP and T2SL both use mesa technology where pixels are defined by ICP etching. Due to polarization selection rule, the QWIP material system needs grating and mirror which is formed by ICP etch followed by deposition of the contact metal. On the other hand, T2SL requires only metal deposition on top of the pixel to serve the top contact as well as a mirror (Figure 2).

The manufacturing process for T2SL requires an extra step of passivation before encapsulation of the pixels to minimise surface recombination and thus reduce dark current. QWIP, however, does not require any passivation due to inherent technology based on majority carriers.

In both processes, through the opening of the Via after encapsulation, the UBM is deposited as final step of processing. The wafer is diced and detector chips are prepared for hybridization with defined cleaning steps. Hybridisation process details are given in the section below. Further details of the complete FPA fabrication process can be found in our earlier works presenting production status of QWIPs [3] and T2SLs [6] based infrared photodetectors at IRnova.

Despite these differences in the architecture and epitaxial properties, there is much similarity in the processing techniques used in both QWIP and T2SL wafer manufacturing which means we have the advantage of using the same production line for both.

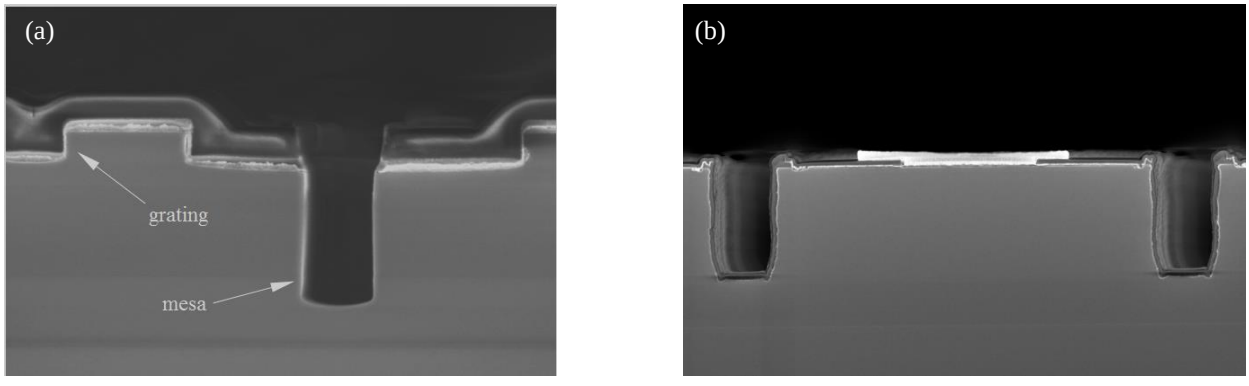

Figure 2: SEM cross-section images of a (a) QWIP pixel (b) T2SL pixel

2.2. Hybridization process for 15µm pitch 640MW/LW FPA's

IRnova flip-chip bond 15µm pitch 640 × 512 pixels FPA's in IRnova's own advanced flip-chip bonder FC300 from SET. The diced chips are flip-chip bonded individually in the FC300 after reflow treatment of the ROIC chip's indium bumps. The flip-chip bonding process is thermal compression. The thermal compression process is flip-chip bonding with temperatures around 100°C and rather low force. After flip-chip bonding, room temperature operability measurement is done to evaluate the connectivity of the flip-chip bonding process.
Underfiller is dispensed between the chips and the FPA is mounted on a ceramic carrier. After curing of the epoxy the complete substrate removal is done in ways that only the detectors epitaxial layers are left on top of the ROIC chip, and thus with very high yield operation.

2.3. IDDCA integration

In order to complete IDDCA, FPA (QWIP or T2SL) are integrated into the same generic dewar designed by i3system. Cold shield is designed and fabricated with internal black coating and outer reflective coating. Baffles for eliminating stray light are also designed for required F number. A 40 pin feedthrough unit is used for connection of FPA with electronics. Window housing with Ge window is used for final encapsulation. Totally, dewar components are designed for high cooling efficiency and robustness for environment condition. Fabricated DDA (Detector Dewar Assembly) was integrated with a Stirling type 0.5W cooler which led to the completion of IDDCA (Integrated Detector Dewar Cooler Assembly). The MTTF of the IDDCA is guaranteed higher than 15000 hours in operating mode. **Figure 3** presents IDDCA with and without proximity electronics boards.

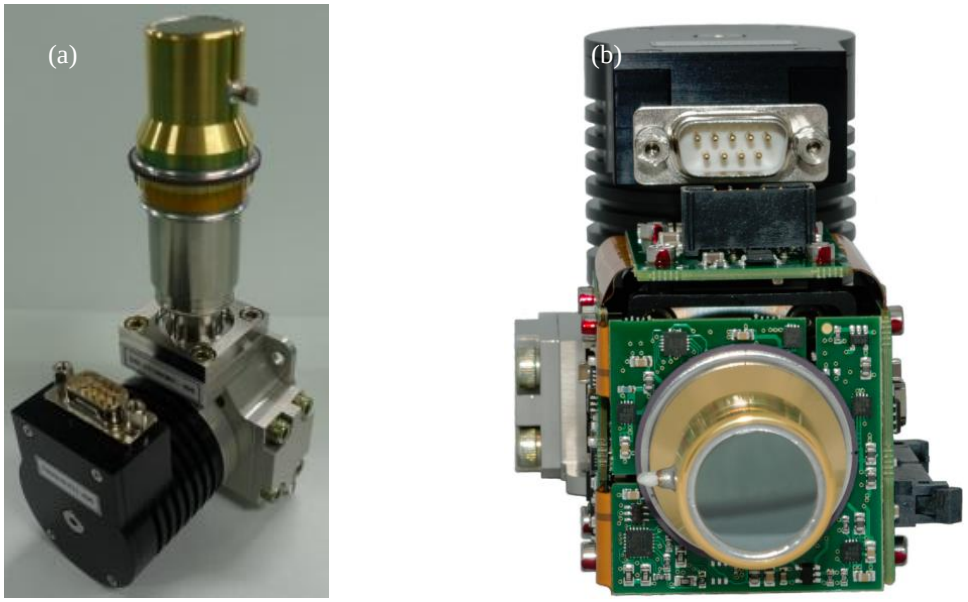

Figure 3. (a) IDDCA without proxy-board b) IDDCA with proxy-board

Both of our MWIR and LWIR detectors make use of a common Readout Integrated Circuit (ROIC) (FLIR indigo's ISC0403). Further to these, as both MWIR & LWIR FPAs make use of same ceramic carrier, cryo-cooler and Dewar assembly, this provides the customer with the choice to select between MWIR and LWIR IDDCA depending on the technical requirements and these replaceable cores can be mounted in similar camera systems with similar electronics. Further to this the possibility to integrate similar sized FPAs and Dewar assembly provides the flexibility to select other functionalities like different F-number depending on the application.

3. RESULTS

3.1 IRnova 640-LW IDDCA performance: NETD, MTF, FPN & Stability

The performance of the integrated image sensors on the FPA level was presented in a previous publication [3]. In this study, the QWIP performance on the IDDCA level is presented. The presented results were measured in two different configurations, on the IDDCA level with a proximity electronic card only and on the camera level. The used demonstrator camera has an additional electronic board for digital signal processing.

Temporal NETD

In **Figure 4(**a) the measured pixel NETD and the corresponding integration time are presented. The temporal NETD on the IDDCA level corresponds to the measured results on the FPA level. At 69 K detector temperature the NETD is 31.3 mK. The integration time is 6.8 ms which makes the IDDCA's compatible with 120 Hz frame rate applications. The integration time is set at the 96 % of saturation against a 50 °C black body. In **Figure 4**(b) the responsivity of the detector in mV/K for different temperatures is shown. For each measurement point the integration time is given in ms.

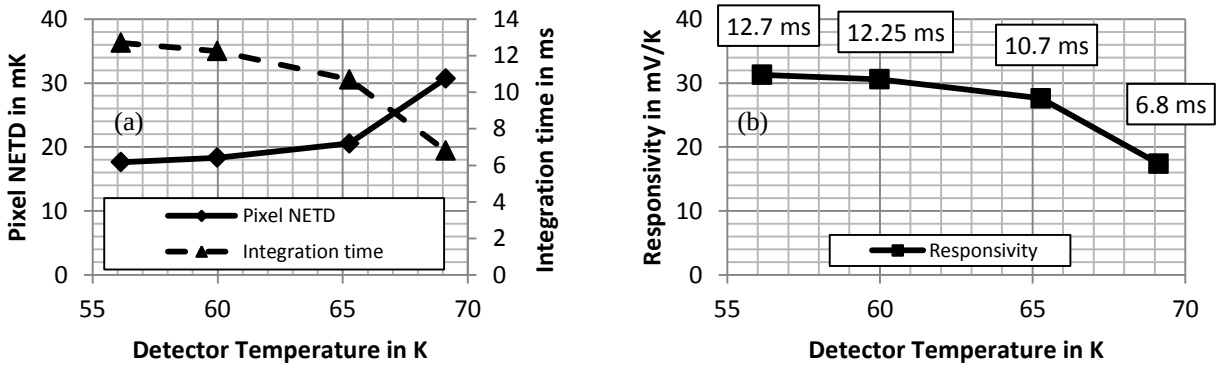

Figure 4. (a) pixel NETD in mK and (b) responsivity in mV/K of the detector for different temperatures

In **Figure 5** the gain correction map shows the uniformity of two different detectors on IDDCA level. The image contrast is adjusted by histogram stretching saturating the upper 1% and the lower 1% of the pixels. The detector temperature is set to 70 K.

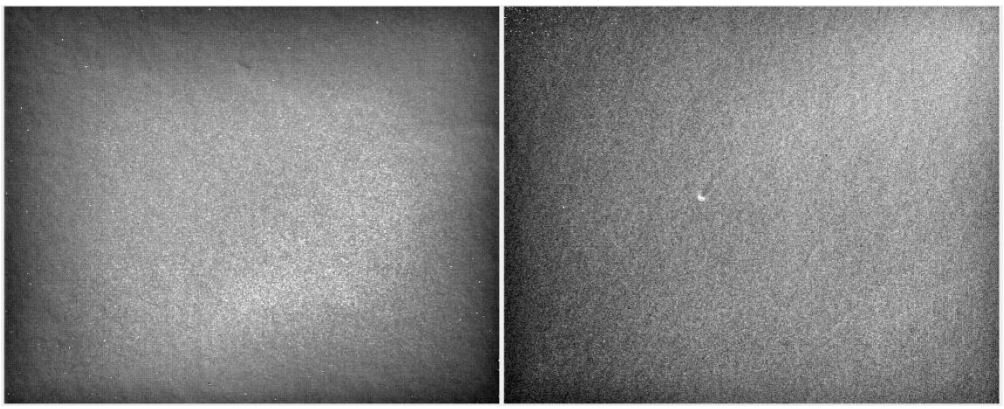

Figure 5. Gain correction map for two different detectors at 70 K; grey scale is +/- 5% of average.

The ISC0403 ROIC allows for overdriving the detector bias range using the Vdet_adj input. With a floating Vdet_adj the bias range varies from ca. -400 mV to +270 mV. However, the used QWIP structure requires a bias voltage in the range of ca. -1V. With Vdet_adj set on 1V level the available voltage range can be moved to about -1200 mV to -460 mV. **Figure 6** shows a bias sweep with Vdet_adj on 1 V voltage level. For different bias voltages the pixel NETD and the used integration time are given. The integration time is limited to 16 ms for 60 Hz frame rate applications compatibility. It is set by increasing the signal to 96 % of the maximum value against a 50 °C black body. The detector is operating at 65 K integrated into an F/2 IDDCA and shows a NETD in the range of 20 mK (**Figure 6**). The overdrive possibility of the ISC0403 ROIC allows for further performance optimization of the detector.

Absorption and Collection Efficiency

Even if the absorption remains the only relevant parameter for QWIP, nevertheless it is interesting to estimate at which bias the highest collection efficiency is reached, a simple way to do it is to follow the response normalized by the corresponding integration time. **Figure 7** shows the normalized response in mV/K/ms as a function of the applied detector bias voltage. As expected by design the normalized response reaches the saturation above 1V.

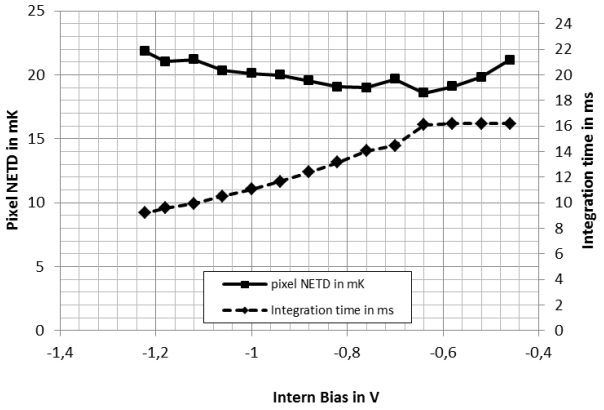

Figure 6 Pixel NETD at 65K K as function of the bias voltage; integration time is limited for 60 Hz frame rate.

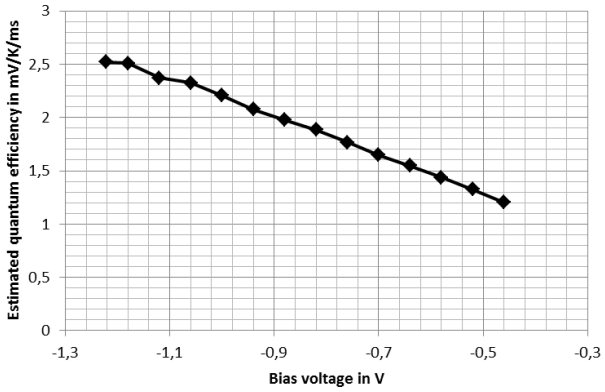

Figure 7 The estimated collection efficiency given in mV/K/ms versus the bias voltage.

Residual Non-Uniformity (RNU)

To evaluate the detector stability the global and local RNU are calculated on a time series of 90 minutes. The calculation does not take into account non-operating pixels and was performed on non-uniformity-corrected images. The spatial core for the local RNU is a 5x5 pixel section. The RNU normalized by the temporal NETD gives an estimation of the detector stability, assuming that the non-uniformity-correction (NUC) stability is good for values below 0.5.

Figure 8 shows the performance stability of an IRnova 640-LW IDDCA over a runtime of 90 minutes. The upper diagram shows the local and the global RNU at the same scale. The both diagram below give a detailed view on the local and global RFPN.

Further the image correctability is evaluated. A 2-point-NUC is applied with calibration values at 35 and 55 °C. The RFPN normalized by the NETD is given for corrected images taken with different black bodies in front of the detector. As expected the curve in **Figure 9** shows a W-form typical for this measurement. At 35 and 55 °C RFPN tends against zero, meaning the best correctability. After the first measurement at t=0 (T0) the measurement was repeated for two additional cooling down cycles over 2 days. For all three cooling down cycles the RFPN normalized by NETD is below 0.4 in the temperature range of interest.

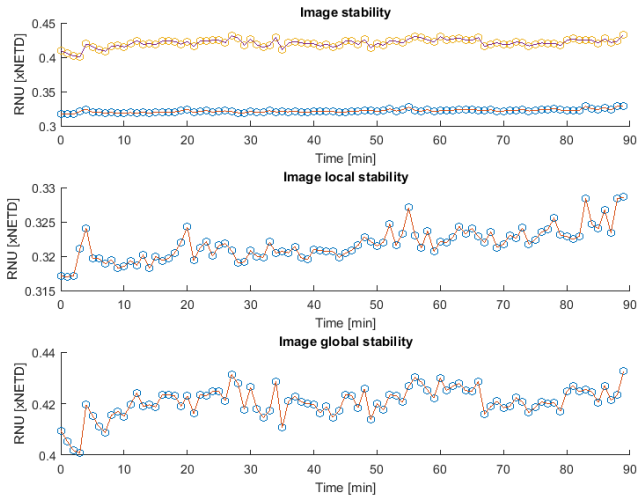

Figure 8. Residual non-uniformity normalized by the NETD for a measurement cycle of 90 minutes. From top to bottom: local and global image stability in the same scale; local stability; global stability.

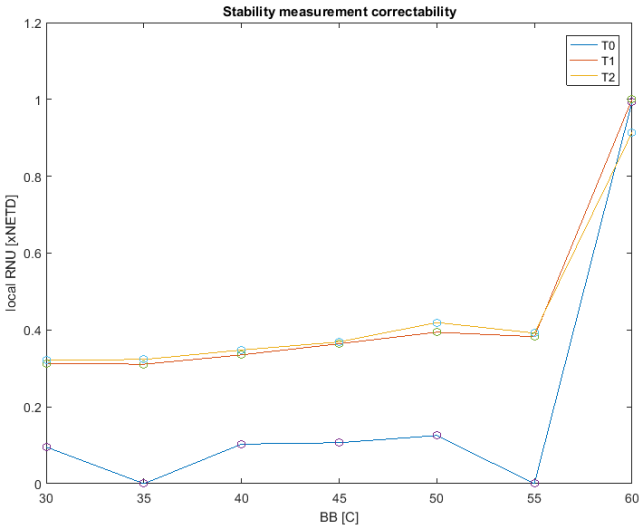

Figure 9. Local RNU is given normalized by the NETD showing the NUC stability for three cooling down cycles.

Another way to illustrate the stability of the NUC maps for the detector is given in **Figure 10**.

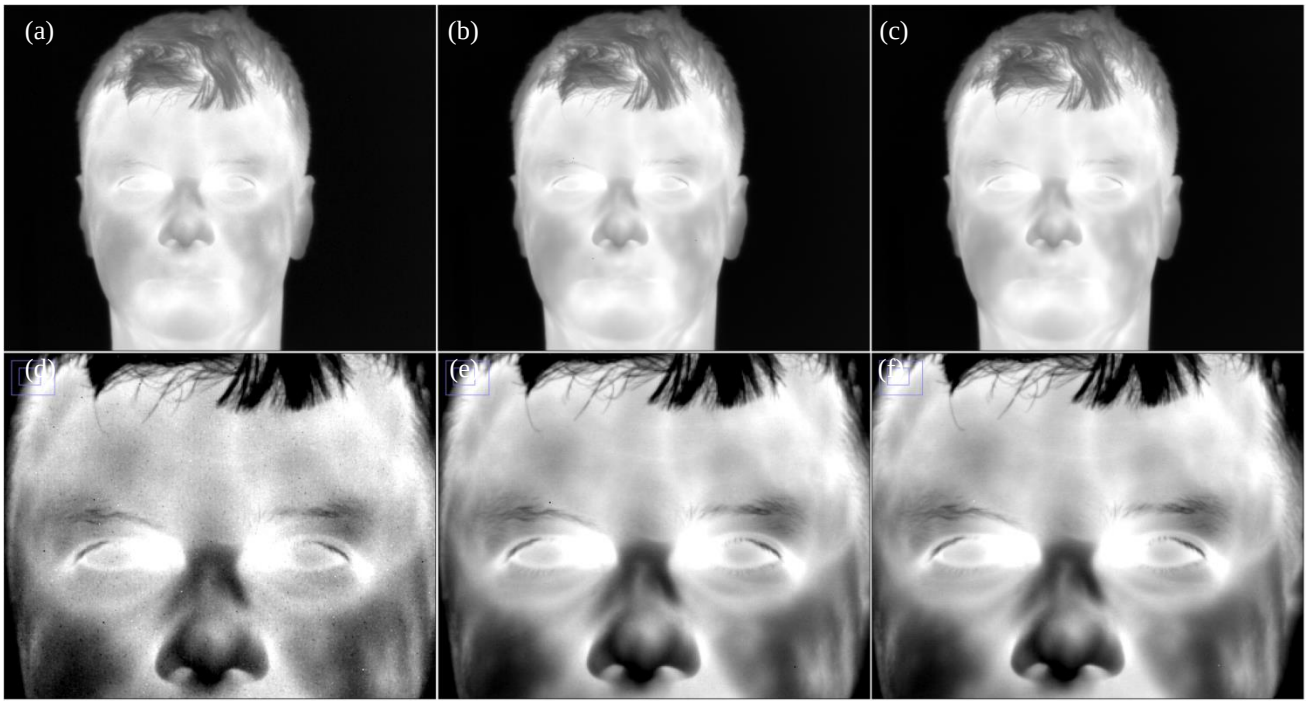

Figure 10. (a) QWIP image corrected using a 6 month old gain and offset map (b) image corrected with a 6 month old gain map but a current offset map (c) image with a current 2-point correction. For a), b) and c) the grey scale is spread over 6.5K. (d) image corrected using a 6 month old gain and offset map (e) image corrected with a 6 month old gain map but a current offset map (f) image with a current 2-point correction. Images d), e) and f) show an area zoomed in by 200 % and are overdriven in contract to highlight the spatial noise, the grey scale is therefore spread over 2.5K.

MTF

The MTF measurements for the detector were performed on a basic and simple camera level, **Figure 11**. The camera uses a 50 mm F/2 lens from StingRay with a wavelength range from 8 to 12 µm. A slanted edge method is used to evaluate the MTF performance. The detector temperature of 68 K is used with an integration time of 5 ms and a 2-point-correction with calibration points at 100 and 110 °C. The target temperature is 105 °C. For the modeling of the MTF of the StingRay lens an ideal diffraction limited system is assumed. The cutoff wavelength for the entire system is set to 9µm considering the transmission level of the lens and the spectral response of the detector. It is important to notice that for spatial frequencies higher than 20cycles/mm the lens performance starts to deviate from ideal behavior, which implies that the calculated MTF of the detector is pessimistic. For detectors Nyquist frequency of 33.3 cycles/mm the detector MTF is then demonstrated to be higher than 0.35.

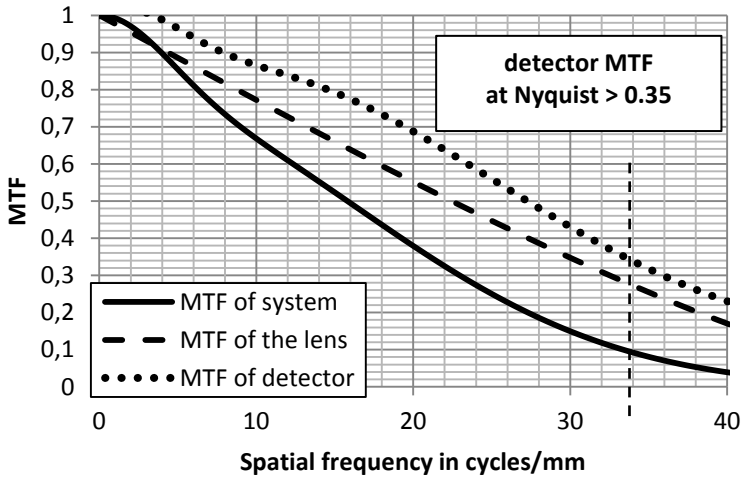

Figure 11. MTF of the detector (dotted line) calculated from a MTF measurement on camera level (solid line) and a MTF of a diffraction limited system (dashed line).

Cooler Power

The highest power consumption of 10.5 W for an IDDCA was measured during the cool down even for a set point temperatures low as 56 K. Once the working temperature is reached, the power consumption does not exceed 9.5 W as shown in **Figure 12**. For the targeted working temperature of 70 K the cooler consumption does not exceed 7 W and is typically 6.8 W.

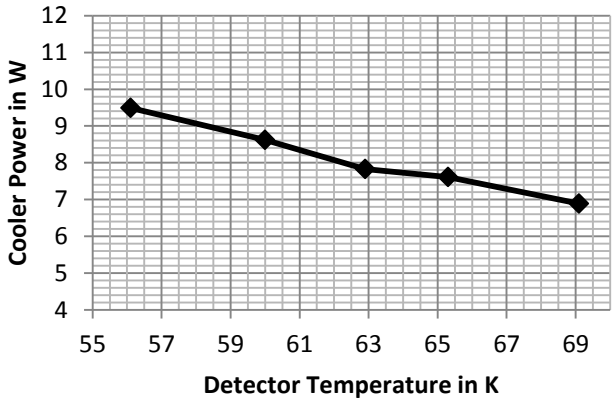

Figure 12. Power consumption of an IDDCA module in steady state versus detector temperature.

3.2 IRnova 640-MW IDDCA performance: NETD, MTF, FPN & Stability

On the FPA level the measurements are made in a test setup using an active pumping assembly which has a cooler integrated in the same way as it is used in IDDCA's. The test setup allows for using different filters and cold shields, which for example can be used for characterization with different apertures. The presented results on the IDDCA level are made with a F/4 aperture in an assembly optimized for 80 K working temperature.

Temporal NETD

Figure 13 shows the measured pixel NETD and the corresponding integration time for both F/2 and F/4 configurations. The integration time is set at the 96% of saturation against a 50 °C black body and is compatible with 60 Hz applications. In lab conditions these detectors shows a NETD of approximately 20 mK with integration times in the range of 2 to 3 ms. This allows for very high frame rates and slow motion applications..

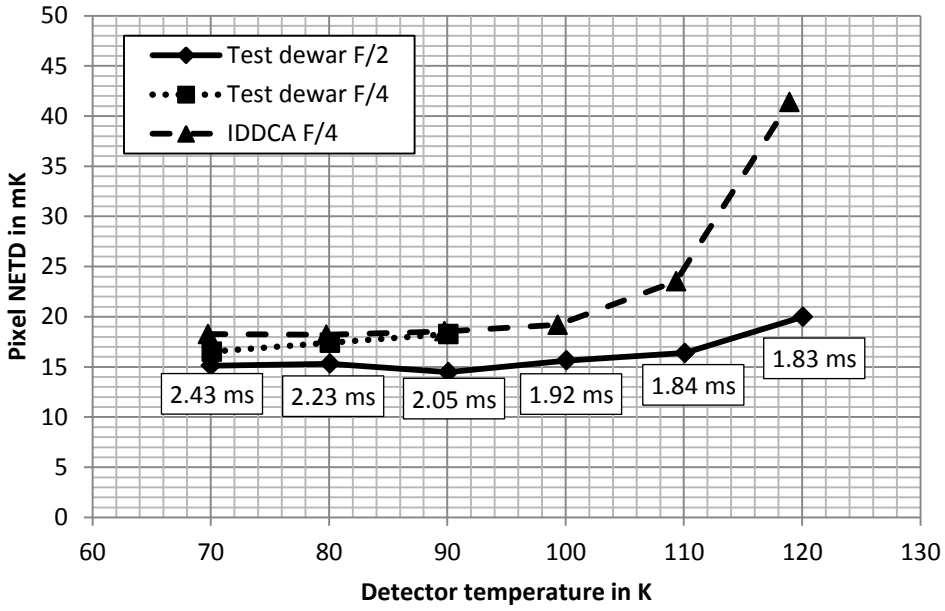

Figure 13. Pixel NETD on IDDCA and test dewar level

Quality picture and NUC stability

Figure 14 demonstrates at the picture level the performance the 640 MW IDDCA. On the left an F/2 IDDCA operating at 80K was used to make a picture at ca. 0 °C outdoor temperature (Nordic weather…). On the right an F/4 IDDCA is used to capture one of the authors in laboratory temperature environment. The detector temperature is 120 K and the integration time is 10 ms. Both pictures are corrected on the camera level using simple 2-point-NUC. In case of the outdoor picture a 10 days old gain map is used.

Figure 14. IRnova640 MW performance demonstration. (a) Stockholm quayside at ca. 0 °C outdoor temperature; 80 K detector temperature,. (b) One author in room temperature environment; 120 K detector temperature, 10 ms integration time, F/4 aperture.

4. CONCLUSIONS

In this paper we have demonstrated the capability of both T2SL and QWIP to meet the most demanding requirements of next generation and emerging infrared sensing applications. Manufacturing processes maturity enabled highly sensitive and state of the art uniformity all at a controlled cost.

5. ACKNOWLEDGEMENTS

Authors would like to express their gratitude towards the Process group and the Optronics group at IRnova for providing processing assistance and for performing a comprehensive set of measurements, without forgetting Daniel and Sergiy for the last touch.

REFERENCES

[1] Henk Martijn, Anders Gamfeldt, Carl Asplund, Sergiy Smuk, Himanshu Kataria, Eric Costard, "QWIPs at IRnova, a status update", Proc. SPIE 9819, 981918 (2016)

[2] Linda Höglund, Carl Asplund, Rickard Marcks von Würtemberg, Himanshu Kataria, Anders Gamfeldt, Sergiy Smuk, Henk Martijn, Eric Costard, "Manufacturability of type-II InAs/GaSb superlattice detectors for infrared imaging", Infrared Physics and Technology, Vol. 84, August 2017.

[3] Himanshu Kataria, Carl Asplund, Anton Lindberg, Sergiy Smuk, Jörgen Alverbro, Dean Evans, Susan Sehlin, Smilja Becanovic, Pia Tinghag, Linda Höglund, Fredrik Sjöström, Eric Costard, "Novel High Resolution VGA QWIP detector", Proc. SPIE 10177, Infrared Technology and Applications XLIII, 101772C (3 May 2017).

[4] Alexandru Nedelcu, Hugues Facoetti, Eric Costard, Philippe Bois, "Small pitch, large format long-wave infrared QWIP focal plane arrays for polarimetric imagery", Proc. of SPIE Vol. 6542, 65420U, (2007)

[5] Nedelcu Alexandru, Hamon Gwénaëlle, Digonnet Adrien, Mathonnière Sylvain, Brière de l'Isle, "Low pitch LWIR QWIPs: Performance level and image quality", Infrared Physics & Technology 70 (2015) 129–133

[6] Linda Höglund, C. Asplund, R. Marcks von Würtemberg, A. Gamfeldt, H. Kataria, D. Lantz, S. Smuk, E. Costard and H. Martijn, "Advantages of T2SL – Results from production and new development at IRnova", Infrared Technology and Applications XLII, 98190Z (20 May 2016).